Flexural behaviour and theoretical prediction of lightweight ferrocement composite beams

Case Studies in Construction Materials 9 (2018) e00204

Contents lists available at ScienceDirect

Case Studies in Construction Materials

journal homepage: www.elsevier.com/locate/cscm

Case study

Flexural behaviour and theoretical prediction of lightweight ferrocement composite beams

Ibrahim G. Shaaban[a,*,1], Yousry B.I. Shaheen[b], Essam L. Elsayed[c,2], Osama A. Kamal[d], Peter A. Adesina[e,3]

[a] Department of Civil Engineering and Industrial Design, University of Liverpool, United Kingdom
[b] Civil Engineering Dept., Menoufia University, Shebin Elkoum, Egypt
[c] Benha University, Shoubra, Egypt
[d] Civil Engineering Dept., Benha University, Shoubra, Egypt
[e] Department of Civil Engineering and Industrial Design, University of Liverpool, UK

ARTICLE INFO

Article history:
Received 21 July 2018
Received in revised form 16 September 2018
Accepted 28 September 2018

Keywords:
Ferrocement composite beams
Reinforcement mesh types
Core material type
Post crack stiffness
Energy absorption
Theoretical modelling

ABSTRACT

Sixteen full-scale simply supported composite beams of the same dimensions, breadth = 100 mm, thickness, 200 mm, and length of 2000 mm, subjected to flexural loading, were experimentally tested and their structural parameters, namely, pre-crack stiffness, serviceability loads, post-cracking loads, energy absorption, ultimate load-to weight ratio, and compressive strains were investigated. In addition, theoretical prediction of ultimate loads was carried out to adopt a theoretical approach as a design methodology for ferrocement elements. Experimental results showed that pre-crack stiffness, maximum service loads, maximum values of energy absorption and ultimate loads to weight ratios of ferrocement beams are higher than that of lightweight control beam by up to 46%, 32%, 64.4% and 32.8%, respectively. Higher post-cracking loads were exhibited by beams reinforced by expanded metal mesh, compared to those reinforced by welded wire mesh regardless of the core filling type. For post cracking load indicator, confinement with expanded metal mesh was the decisive factor affecting the post-cracking load capacity. Beams reinforced with expanded metal mesh showed higher energy absorption than those of the other beams reinforced with welded wire mesh or fiberglass mesh. Increasing the amount of mesh reinforcement results in higher energy absorption for beams made of Autoclaved Aerated Lightweight Brick Core (AAC). Generally, the maximum compressive strains of the ferrocement composite beams were generated at higher loads compared to those of the control beams. Theoretical calculations, based on the assumption of strains and forces distribution block, results in acceptable prediction of the ultimate loads. The ratio of experimental to theoretical ultimate loads ranges from 0.91 to 1.26. This study showed that ferrocement composite beams may be used as an alternative to traditional reinforced normal or lightweight concrete beams after careful choice of the combination of core and mesh types to suit the application in question.

* Corresponding author.
E-mail addresses: Ibrahim.shaaban@liverpool.ac.uk (I.G. Shaaban), ybishaheen@yahoo.com (Y.B.I. Shaheen), essam_labib006@yahoo.com (E.L. Elsayed), Osama.ahm.Kamal@gmail.com (O.A. Kamal), greatpetson121@gmail.com (P.A. Adesina).
[1] On Sabbatical, Benha University, Egypt.
[2] Now working in Concrete and Bridges Testing, Industrial Private Sector, Canada.
[3] Now working with Ove Arup.

https://doi.org/10.1016/j.cscm.2018.e00204

1. Introduction

Ferrocement is a composite construction material which has received increased attention as it offers high quality characteristics in terms of strength, toughness, crack control and impact. This is essentially due to the close spacing and uniform distribution of reinforcement within the material [1–5]. One main distinguishing benefit of ferrocement is that it can be moulded into a wide range of shapes (the mesh reinforcement can be tailored to any required shape), properties (may be metallic or non-metallic, continuous or discrete fibres) and value (affordable or expensive) to meet customer's demands and budget. Ferrocement was designated by Lalaj et al. [4] as a material with enhanced strength capacity and failure mode, which prevents sudden brittle failure and therefore exhibits increased ductility. This material can be a potential roofing material and it has been used for several different applications [6,7]. Ferrocement offers the possibility of producing relatively light prefabricated structural elements, up to 70% of the traditionally reinforced concrete elements, which can be formed into interesting architectural elements for low-cost housing. As a versatile material, ferrocement has been used for the production of prefabricated components required in building construction [3]. Research investigations into the use of ferrocement for the strengthening of structural elements have reported great potential [8–10]. According to Al-Rifaei and Hassan [11] the behaviour exhibited by channel shaped ferrocement elements makes them suitable for the construction of horizontally spanning elements subjected to one-way bending. Developing ferrocement into novel lightweight sandwich structural element for applications in building construction potentially opens new possibilities for sandwich construction in the building industry [12]. Lightweight sandwich structural elements offer high strength-to-weight ratio and quality thermal insulation characteristics [13]. The strength and structural behaviour of voided ferrocement channels investigated by Chandrasekhar et al. [14] showed that though lower flexural strength was exhibited by the channels, a compensation for the reduced strength was offered by the weight reduction in the voided ferrocement channels.

Shaaban [15] investigated the feasibility of ferrocement as a permanent formwork and to improve structural behaviour of flexural reinforced concrete beams. He concluded that using expanded wire fabric as a permanent formwork and adding wings tailored by the same fabric resulted in increased load capacity of the beams by 20% and reduced the crack widths by 35%. In addition, Abdul Kadir et al. [16] studied ferrocement as permanent formwork for reinforced concrete beams. They incorporated mechanical shear connections between the ferrocement forms and the concrete cores. The results showed that ferrocement formwork contributed about 16–75% to the flexural strength of the composite beams. The concrete beams which incorporated shear connectors exhibited a 10% increase in strength, and a reduced overall deflection when compared with those without shear connectors. Abdel Tawab et al. [17], investigated the viability of precast permanent U-shaped ferrocement laminates of different types of mesh reinforcement. They reported high serviceability and ultimate loads, crack resistance and good impact resistance from the use of the ferrocement formwork. The study was further continued by Fahmyet al. [18] who applied the ferrocement concept in the development of reinforced concrete beams made of precast permanent U-shaped reinforced mortar forms which encase different core material types as viable alternative to traditional reinforced concrete beam. They used different types and amount of mesh reinforcement layers for the U-shaped permanent forms. They also used different core material types to achieve extra lightweight elements. Adhesive bonding layer and mechanical connectors were used as shear connections between the core material and the precast permanent reinforced mortar form. The results from the experimental work validated their proposed system as having better crack behaviour, high serviceability and failure loads, and good energy absorption. Since the self-weight of structural elements with high density accounts for a significant portion of total load sustained by a structure, adopting approaches which will reduce the self-weight of the structure offers reduction in structural element's cross-section, foundation size, overall cost and susceptibility to failure caused by vibration and earthquake forces.

2. Research objectives

This study is the phase II part of a larger research program focusing on the ferrocement composite beams. In Phase I [19], the effect of various core materials and reinforcement mesh types on some structural indicators such as first crack loading, ultimate load, corresponding deflections and ductility of specimens were studied. This paper is a continuation of the experimental work reported by Shaaban et al. [19] and will be focusing on other structural characteristics including pre-crack stiffness, post-cracking load, service loads, energy absorption, ultimate load-to-weight ratio, and compressive strain of specimens. In addition, theoretical prediction of the experimental ultimate loads was carried out using stress and strains blocks. The main aim of these two papers is to achieve a better understanding of the true behaviour of lightweight ferrocement composite beams. This may help in exploring the possibility of using lightweight ferrocement composite beams as alternatives to conventional reinforced concrete beams.

3. Experimental program and test setup

Sixteen simply supported composite beams of the same dimensions, breadth = 100 mm, thickness, 200 mm, and length of 200 0 mm were prepared. Configurations, were as reported by Shaaban et al. [19] and seen in Fig. 1. They were classified into four different groups. The first is the control group, A, the other three groups, B, G, and F, each having a different core filling, namely Autoclaved Aerated Lightweight brick core (AAC), Extruded Foam Core (EFC) and Light Weight Concrete Core (LWC), respectively. Beams A1 and A2 were the conventional control concrete beams which formed Group A. Beams in Groups B, G

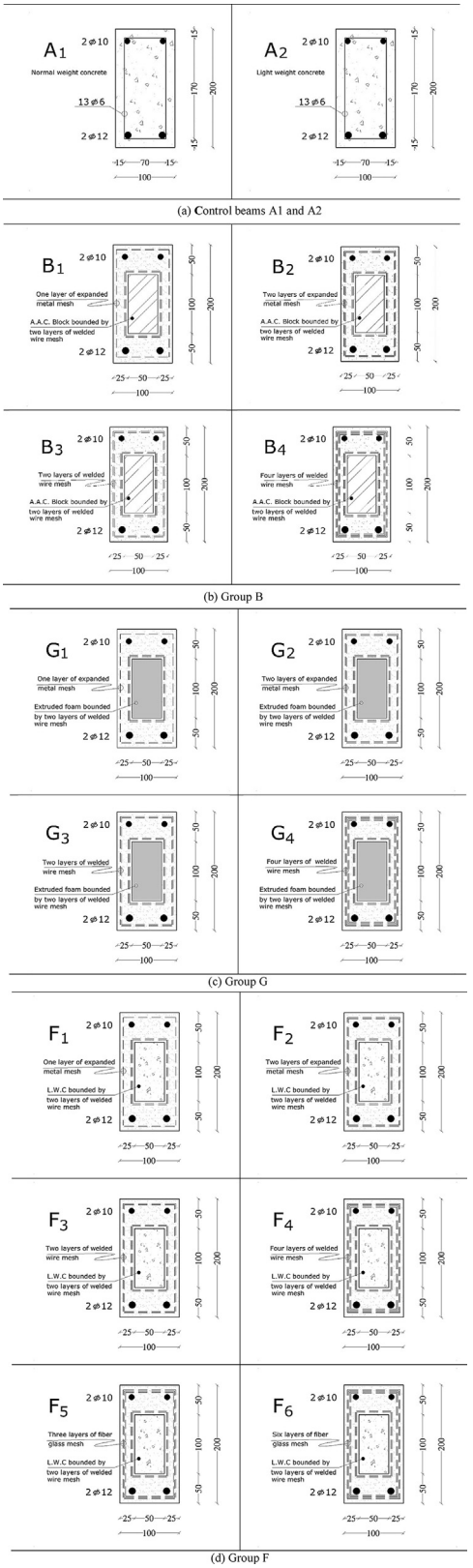

(a) Control beams A1 and A2

(b) Group B

(c) Group G

(d) Group F

Fig. 1. Typical cross sections of test specimens [19].

and F were reinforced with expanded metal mesh, welded wire mesh and fiberglass mesh of different amounts of mesh reinforcement (see Fig. 1). The final dimensions of the ferrocement beams were the same as the control beams regardless of the amount of mesh reinforcement (see Fig. 2a). One-point loading system with a span of 1800 mm force was used for testing the flexural behaviour of the beams. Linear Variable Displacement Transducer (LVDT) placed at mid span of test beam was used to monitor deflection at the point of load application. Two PI gauges placed at 2 cm away from top and bottom edges of the test beam at mid span were used to measure concrete strain. Fig. 2b shows the setup and dimensions of a typical tested beam. A small load is then first applied to make sure that all instruments were working. The load is thereafter increased gradually till the failure of the specimen. At each load stage, strains in concrete and the deflections were recorded automatically using a computerized data acquisition (DAQ) system. The crack pattern was also noted at each load stages. The ultimate load is identified when excessive cracking occurs at the bottom of the beam, applied load drops and deflection increases according to El-Wafa and Fukuzawa [12]. Details of mix proportions, mesh reinforcement, stages involved in the casting of the beams, and details of testing, including strains in concrete, recorded deflections and crack pattern noted at each load stage, are explicitly described by the authors in phase I [19].

4. Experimental results and discussion

The full response of load-deflection relationships for reinforced concrete beams is normally divided into three specific regions, namely, a linear region before yield (pre-crack stage); a transition region with gradual yield (multiple cracking stage); and a region of full plastic deformation which ends with ultimate failure (post-cracking stage) [18,19]. The load deflection relationships are shown in Fig. 3 and they were studied in detail in phase I [19]. Structural indicators, namely, pre-crack flexural stiffness, serviceability loads, post-cracking load, energy absorption, ultimate load-to-weight ratios, and recorded compressive strains, were observed from crack pattern (see Fig. 4) and were calculated from the load deflection and compressive strain relations shown in Figs. 3 and 5. These structural indicators are studied in the following sections and presented in Table 1. The effect of core material types, mesh reinforcement types and number of mesh layers on these structural indicators are discussed herein for the studied lightweight ferrocement concrete composite beams. The different weights of studied specimens after curing are reported in Table 2. The average weights of ferrocement composite beams with lightweight cores were lower than that of the conventional normal weight concrete beam A1 by 17.7%, 27.3% and 22.5% for AAC, EFC and LWC cores, respectively.

4.1. Pre-crack flexural stiffness indicator

The pre-crack flexural stiffness indicator was studied to check the sensitivity of different combinations of lightweight cores, and different types and amount of mesh reinforcement at various stages of loading starting from a low level of loads. Pre-crack flexural stiffness indicators were calculated as the ratio of the first crack loads of test beams to their first crack deflection. The different values of pre-crack flexural stiffness indicator of the studied beams are presented in Table 1. Fahmy et al. [18]; El-Wafa and Fukuzawa [12] reported similar pre-crack stiffness among their tested beams. It can be seen from Table 1 that pre-crack stiffness indicator values of the beams in the same group showed considerable difference from one

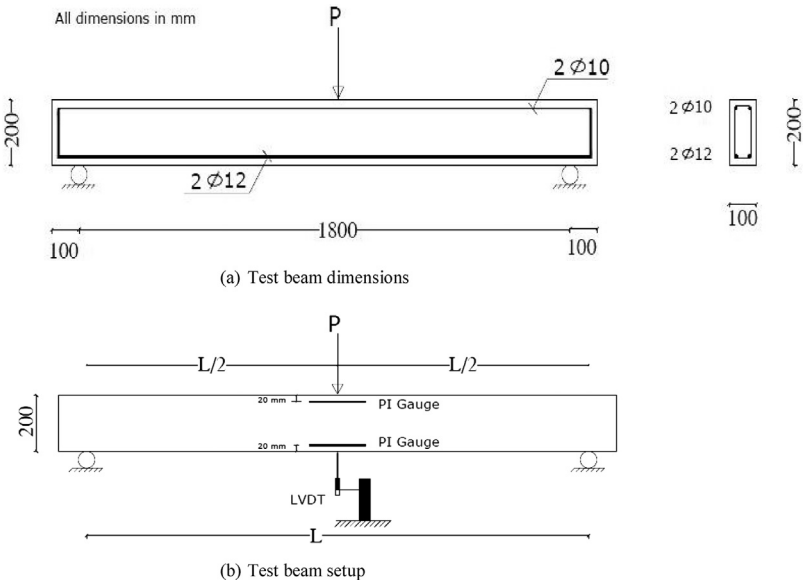

Fig. 2. Typical test beam dimensions and setup [19].

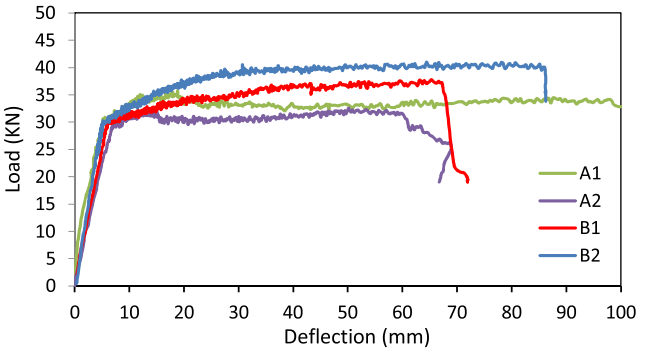

EMM

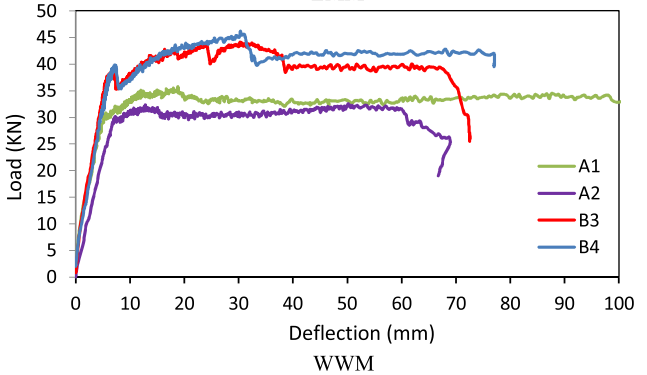

WWM

(a) Group B, beams made of AAC core

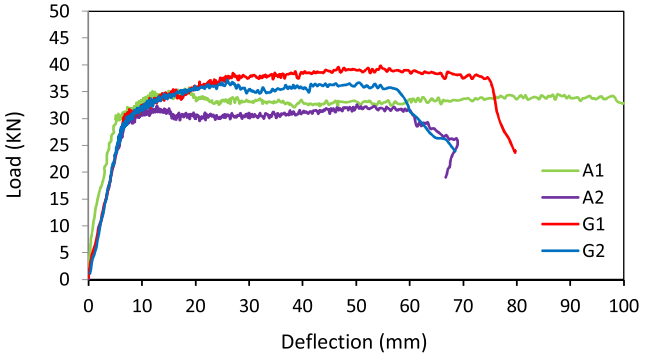

EMM

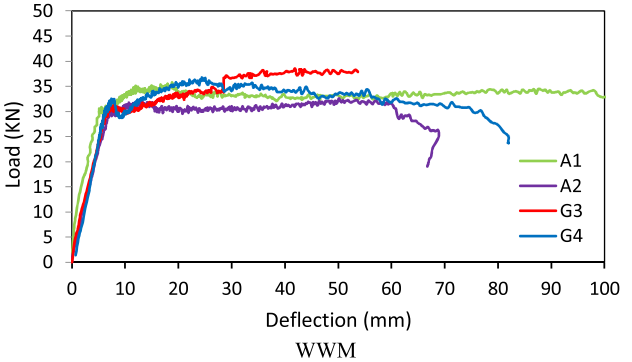

WWM

(b) Group G, beams made of EFC core

Fig. 3. Load-deflection relationships of different groups of test beams [19].

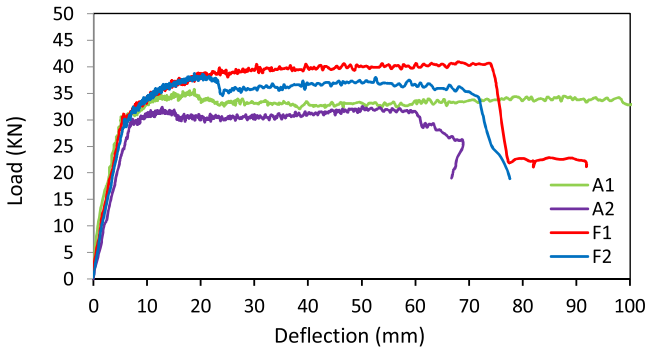

EMM

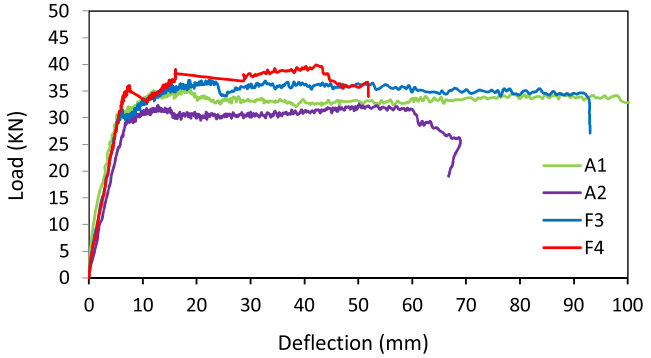

WWM

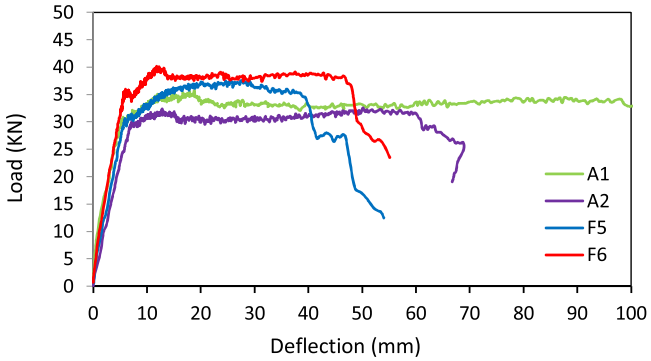

FGM

(c) Group F, beams made of LWC core

Fig. 3. (Continued)

specimen to another depending on studied parameters. For Group A, specimens, Specimen A1 made of normal weight concrete had a pre-crack stiffness indicator value higher than that of the control lightweight specimen A2 by 34%. The higher stiffness can be attributed to the higher Young's modulus and consequently higher bond between concrete and steel in the normal weight concrete matrix compared to its lightweight concrete counterpart [3,7,19]. It can be also observed from Table 1 that most of the studied ferrocement beams exhibited higher flexural pre-crack stiffness indicator values compared to the lightweight control specimen A2 to different degrees depending on core type, mesh reinforcement type and amount.

For Group B specimens of AAC core, the values for Beams B1 (one layer of expanded metal mesh), B2 (two layers of expanded metal mesh), B3 (two layers of welded wire mesh) and B4 (four layers of welded wire mesh) were higher than that of the control lightweight Beam A2 by 14%, 32%, 42%, and 26%, respectively. For Group G specimens of EFC core, the value for Beam G3 (two layers of welded wire mesh) was lower than that of the control lightweight Beam A2 by 3% while the indicators for Beams G1 (one layer of expanded metal mesh), G2 (two layers of expanded metal mesh), and G4 (four layers of welded wire mesh) were higher than that of Beam A2 by 10%, 3.4%, 42%, and 6.5%, respectively. For Group F specimens of LWC core, the indicator values for Beams F1 (one layer of expanded metal mesh), F2 (two layers of expanded metal mesh), F3 (two

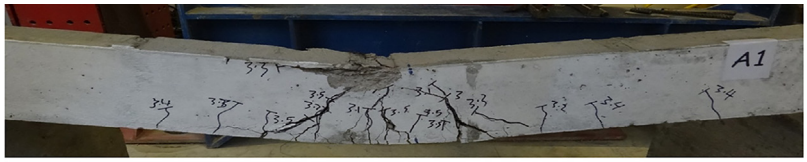

(a) Group A

(b) Group B

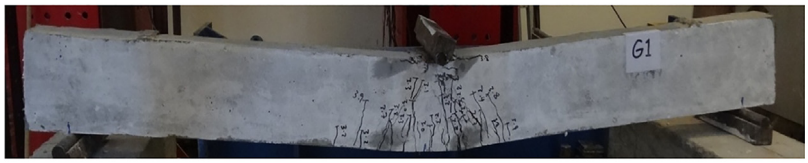

Fig. 4. Crack pattern for different studied test beams.

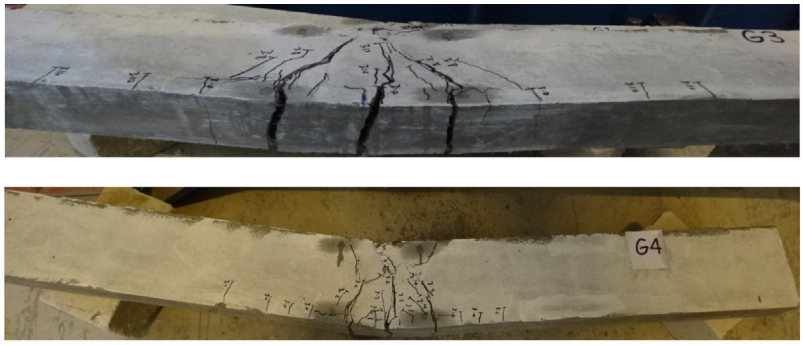

(c) Group G

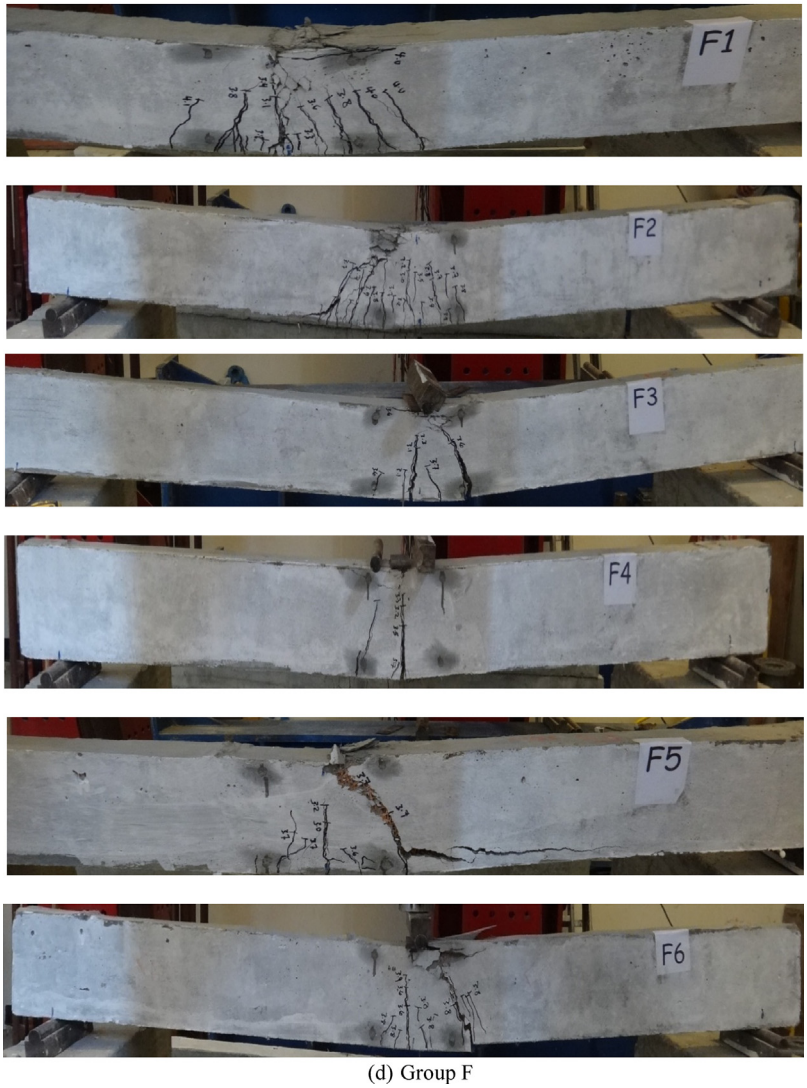

(d) Group F

Fig. 4. (Continued)

layers of welded wire mesh), F4 (four layers of welded wire mesh), F5 (three layers of fiberglass mesh) and F6 (six layers of fiberglass mesh) were higher than that of Beam A2 by 35%, 24%, 24%, 20%, 26% and 46%, respectively. The above values for the change of pre-crack stiffness indicators show that the effect of amount and type of mesh reinforcement is highly dependent on the core type. This agrees with the findings of Fahmy et al. [18] who reported the significance of amount and type of mesh reinforcement and their dependency on the filling core type. The maximum increase in the stiffness indicator was for Beam F6 reinforced by six layers of non-metallic (fiberglass mesh) and LWC core.

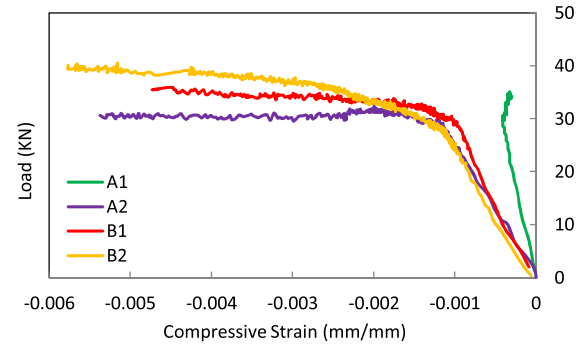

EMM

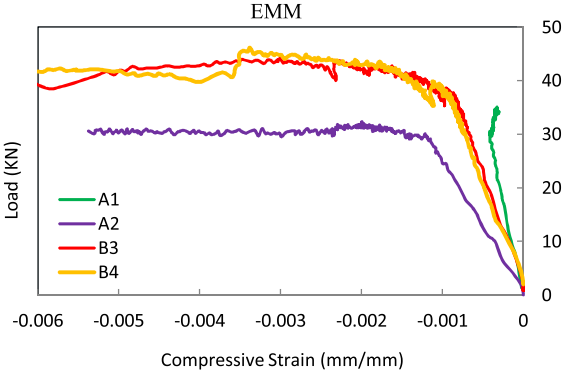

WWM

(a) Group B, beams made of AAC core

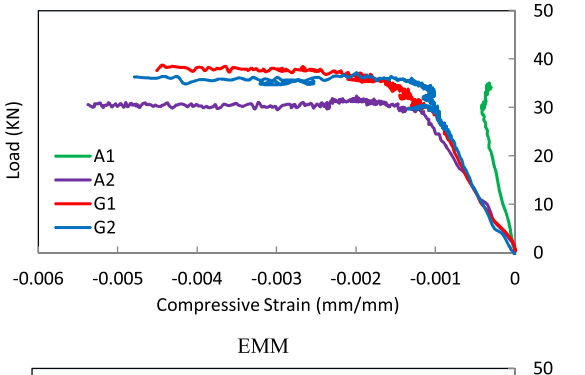

EMM

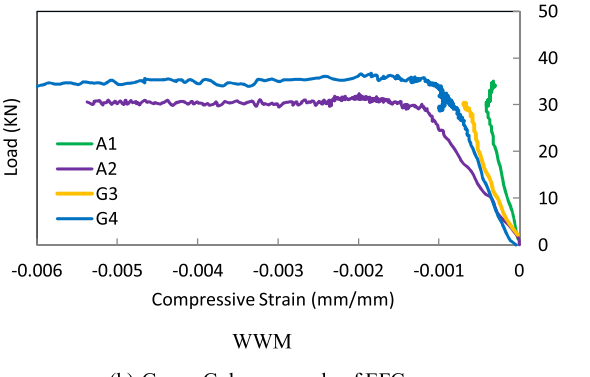

WWM

(b) Group G, beams made of EFC core

Fig. 5. Load-compressive strain relationships for all tested beams.

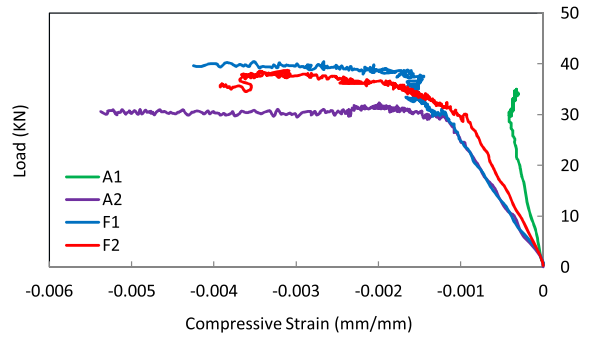

EMM

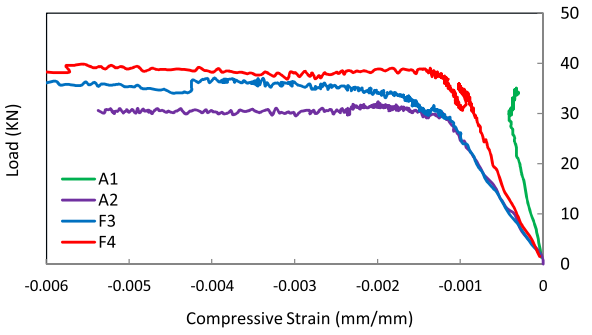

WWM

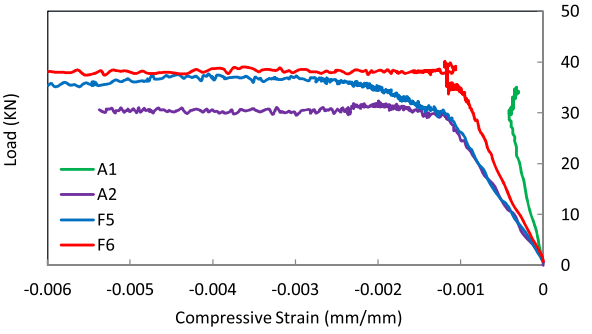

FGM

(c) Group F, beams made of LWC core

Fig. 5. (Continued)

4.2. Serviceability load

The serviceability load is proposed in this investigation as the load corresponding to a deflection equals to span of the beam/350, which is a more conservative deflection limit compared to the limit prescribed by CEN [20]. The performance of studied beams at service loads is normally used to check design serviceability limit states. Table 1 shows that service loads values are close to the first crack loads. Some of the specimens developed first crack before reaching their serviceability loads such as Specimens A1, B1, B2, F1, F2, and F5, while other specimens developed first crack after their serviceability load had been reached. It can be observed from Table 1 that most of ferrocement composite specimens with different lightweight cores exhibit higher serviceability loads than that of the lightweight control specimen. In addition, the specimens reinforced by welded wire mesh or fiberglass mesh showed higher serviceability loads than those reinforced by expanded metal mesh. For example, for beams with AAC core and reinforced by welded wire mesh, B3 reinforced by two layers and B4 reinforced by four layers had serviceability loads higher than that of lightweight control beam A2 by 24% and 32.4%, respectively. For beams with EFC cores and reinforced by welded wire mesh, G3 reinforced by two layers and G4 reinforced by four layers had serviceability loads higher than that of lightweight control beam by only 0.13% and 5.3%, respectively. For beams with LWC cores and reinforced by welded wire mesh, F3 reinforced by two layers and F4 reinforced by four layers had serviceability loads higher than that of lightweight control beam A2 by 1.2% and 18.6%, while beams F5 reinforced by three layers of fiberglass mesh and F6 reinforced by six layers of fiberglass mesh exhibited serviceability loads higher than that of lightweight control beam A2 by 3.4% and 14.1%, respectively.

Table 1
Structural characteristics and prediction of ultimate loads for tested beams.

Specimen group & designation		Weight (kg)	First crack load, kN	First crack deflection, mm	Pre-crack flexural Stiffness indicator, kN/mm	Serviceability load (kN)	Post-cracking load, kN	Ultimate load (kN)			Energy absorption (kNmm)	Ultimate load to weight ratio (kg/kg)
								Experimental, P_{exp}	Predicted, P_{prd}	P_{exp}/P_{prd}		
A	A1	103.8	30.86	5.56	5.50	31.35	5.19	35.76	33.90	1.05	3805.73	35.12
	A2	80.4	30.11	7.32	4.11	30.05	2.45	32.56	31.31	1.04	1955.69	41.28
B	B1	84.0	30.20	6.21	4.70	30.75	7.57	37.77	36.15	1.04	2366.50	45.84
	B2	86.4	29.75	5.49	5.42	31.28	11.23	40.98	36.45	1.12	3214.80	48.35
	B3	83.7	38.52	6.61	5.83	37.23	5.62	44.14	39.97	1.10	2794.48	53.76
	B4	87.5	39.80	7.22	5.16	39.79	6.39	46.19	42.58	1.08	3097.33	53.81
G	G1	74.0	30.79	6.82	4.51	30.48	9.03	39.82	37.96	1.05	2785.87	54.85
	G2	75.0	30.26	7.12	4.25	29.06	6.93	37.19	40.79	0.91	2206.27	50.55
	G3	73.7	31.17	7.83	3.98	30.09	7.33	38.50	35.89	1.07	1764.81	53.25
	G4	79.2	32.51	7.43	4.38	31.64	4.22	36.73	36.66	1.00	2569.69	47.27
F	F1	94.0	31.09	5.60	5.55	31.70	9.86	40.95	32.43	1.26	3187.16	44.41
	F2	92.3	30.13	5.90	5.11	31.42	8.62	38.75	33.21	1.17	2627.52	42.80
	F3	92.1	31.59	6.21	5.09	30.41	5.49	37.08	33.94	1.09	3162.80	41.04
	F4	94.4	35.98	7.32	4.92	35.63	3.89	39.87	32.30	1.23	1807.06	43.05
	F5	90.0	30.60	5.90	5.19	31.07	7.07	37.67	34.36	1.10	1620.24	42.67
	F6	89.2	35.96	6.00	5.99	34.28	4.17	40.13	35.77	1.12	1920.92	45.86

Table 2
Relative weight of specimens after curing [19].

Specimen Designation	A1	A2	B1	B2	B3	B4	G1	G2	G3	G4	F1	F2	F3	F4	F5	F6
Wt. after curing (Kg)	103.8	80.4	84.0	86.4	83.7	87.5	74.0	75.0	73.7	79.2	94.0	92.3	92.1	94.4	90.0	89.2
% Wt. reduction relative to A1	. . . . .	22.5	19.1	16.8	19.4	15.7	28.7	27.7	29.0	23.7	9.4	11.1	11.3	9.1	13.3	14.1

It can be seen from the above values and the results recorded in Table 1 that the type of core, type and number of mesh reinforcement have significant effect on the increase of serviceability loads of ferrocement beams over that of lightweight control beam. The higher service loads exhibited by ferrocement beams may be attributed to the high specific surface and close reinforcement layers, which resulted in lower deflections with tighter crack widths and spacing. It is interesting to find that six layers of fiberglass mesh improved the serviceability loads over that of lightweight control beam by a reasonable value (18.6%). This can be very useful in aggressive environmental conditions which normal metal mesh may corrode. This agrees with the findings of Shaheen and Elsayed [[21]– [24]] who reported higher serviceability loads for ferrocement water tanks compared to tanks built of traditional reinforced concrete. In addition, they reported that the cost of traditional water tanks is four times higher than that of their companions made of ferrocement.

4.3. Post-cracking loads

The post-cracking loads for the studied beams are recorded in Table 1. Post-cracking loads were indicated by the amount of load sustained by a specimen between the period of first crack and ultimate loads. It can be observed that most of ferrocement beams, regardless the type of filling core, sustained higher loads after initial cracking and prior to ultimate failure compared to that of the normal weight, A1, and lightweight, A2, control specimens. The maximum load was observed for B2 reinforced by two layers of expanded metal mesh and it was higher than that of A1 and A2 by 116.4% and 358.4%, respectively. The higher post-cracking loads exhibited by the ferrocement beams can be attributed to their closely spaced mesh layers which, in turn, controlled crack widths and therefore the beams sustained higher load prior to ultimate failure. It can be also observed from Table 1 that beams reinforced with expanded metal mesh, such as B1, B2, G1, G2, F1 and F2, showed higher post-cracking loads compared to those reinforced by welded wire mesh, such as B3, B4, G3, G4, F3, and F4, regardless of the core filling type. This is unlike what was observed for serviceability loads in the previous section which shows the significance of welded wire mesh and core type. These findings may be attributed to the fact that expanded metal mesh has higher flexibility (anisotropic reinforcement not orthotropic like welded wire mesh), which shows higher plastic deformation compared to other mesh reinforcement. This agrees with Shaaban and Seoud [2]; Singh and Talwar [22] who found that ferrocement structural elements reinforced by expanded metal mesh showed higher post-cracking loads compared to those reinforced by welded wire mesh. In addition, ferrocement structures reinforced by expanded metal mesh can resist higher temperature than those reinforced by welded wire mesh [7].

It can be observed from Table 1 that increasing the amount of mesh reinforcement does not necessarily result in a higher post-cracking loads, but it depends on the core filling type. For example, specimens in Group B with AAC core, B2 reinforced

by two layers of expanded metal mesh and B4 reinforced by four layers of welded wire mesh exhibited post-cracking loads higher than those of B1 reinforced by one layer of expanded metal mesh and B3 reinforced by two layers of welded wire mesh by 48% and 13.7%, respectively. On the other hand, Group G specimens with EFC core, G2 reinforced by two layers of expanded metal mesh and G4 reinforced by four layers of welded wire mesh exhibited post cracking loads lower than those of G1 reinforced by one layer of expanded metal mesh and G3 reinforced by 2 layers of welded wire mesh by 23.2% and 42.4%, respectively. For specimens with LWC core, F2 reinforced by two layers of expanded metal mesh and F4 reinforced by four layers of welded wire mesh have post cracking loads lower than those of F1 reinforced by one layer of expanded metal mesh and F3 reinforced by two layers of welded wire mesh by 12.6% and 29.1%, respectively. Specimens with LWC core and reinforced by fiberglass mesh showed the same manner as those with EFC core as F6 reinforced by six layers had post cracking load lower than that of F5 reinforced by three layers by 41%. Previous research works including those of Singh and Talwar [22]; Hassan [23] stated that the additional load sustainable by ferrocement elements at the post-crack stage is dependent on the filling cores and number of reinforcement layers, which controlled crack widths thereby making the beams sustain more load before ultimate failure.

4.4. Energy absorption

The energy absorption values of different beams were calculated as the areas under the load-deflections relationships shown in Fig. 3 and are tabulated in Table 1. It was found that the energy absorption of normal weight control specimen, A1, was almost double as much that of lightweight control specimen, A2. In addition, energy absorption for ferrocement beams were found to be lower than that of the normal control specimen, A1, and, in most cases, higher than that of lightweight control specimen, A2. However, the energy absorption values for specimens reinforced with fiberglass mesh were lower than that of both the normal weight control specimen, A1, and the lightweight control specimen, A2. Regarding groups of ferrocement beams, the highest energy absorption was shared between beams made of AAC (B2, 64.4% increase in energy absorption over that of A2) and LWC cores (F1, 63% increase in energy absorption over that of A2). The minimum energy absorption value was observed for F5 reinforced by three layers of fiberglass mesh (F5 had energy absorption less than that of A2 by 17.1%). Similar to the observations found above for post-cracking loads, beams reinforced with expanded metal mesh showed higher energy absorption than those of the other beams reinforced with welded wire mesh or fiberglass mesh. Higher energy absorption in the beams reinforced with expanded metal mesh can be attributed to the higher plastic deformation and consequently larger area under the load-displacement curve, for these beams [19]. Increasing the number of mesh reinforcement layers resulted in higher energy absorption for beams made of lightweight cores especially for AAC cores. This is in agreement with the findings of El-Wafa and Fukuzawa [12]; Gaidhankar et al. [24]; Shaheen and Eltehawy [25] who reported that energy absorption of lightweight ferrocement structural elements were higher than that of the conventional lightweight reinforced concrete beams.

4.5. Ultimate load-to-weight ratios

The ultimate load-to-weight ratios for studied beams are recorded in Table 1. It can be observed from the table that these ratios for lightweight control beam, A2, and all the ferrocement beams' ratios were higher than that of the normal concrete control beam, A1. In addition, the ferrocement beams' ratios were higher than that of the lightweight control beam to different degrees depending on core type, mesh reinforcement type and amount. The highest ratios were shared among beams made of AAC and EFC cores while the lowest ratio was observed for beams made of LWC cores. For example, the highest increase in the ultimate load to weight ratio for beams in different groups over that of lightweight control beam, A2, were for B4, G1, and F6 and the increase was 30.3%, 32.8% and 11.1%, respectively. This agrees with the findings of El-Wafa and Fukuzawa, [12] who reported higher ultimate load to weight ratios for ferrocement elements than those of traditional reinforced concrete elements. It is worth mentioning that Specimen G1 with EFC core had the maximum ultimate load-to-weight ratio among the ferrocement beams. In addition, as reported above in Sections 4.3 and 4.4, the results in Table 1 shows that increasing the number of mesh layers reinforcement resulted in improvement of the ultimate load-to-weight ratio for beams made of AAC core which means that this type of filling core makes the number of mesh reinforcement layers more significant. Although the unit weight of expanded metal mesh was almost three times that of welded wire mesh, [19], it can be observed from Table 1 that the difference in ultimate load to weight ratios for both of them was not large. This may be attributed to the anisoropy of reinforcement (properties of reinforcement are different in different directions) in expanded metal mesh which can resist cracks in different directions and it can compensate its high weight compared to welded wire mesh which has two perpendincular distinct directions of reinforcement (orthotropic).

4.6. Load compressive strain curves

Fig. 5a–c show the load-compressive strain responses of the studied beams arranged in the three studied groups. It can be seen from these figures that the response for all the studied beams, generally, was almost linear initially followed by a non-linear behaviour. As a result of increasing the applied load to the test beams, when the maximum compressive strain is reached, cracks begin to develop and propagate towards the top surface of the beams. After propagation of cracks due to high

compressive strains, the compressive strain begins to decrease and changes to tensile strain as shown in the crack pattern in Fig. 4. This is similar to the findings of El-Wafa and Fukuzawa, [12]. Tensile strains were studied earlier in phase I while the load-compressive strain relationships are studied in this paper. It was observed from Fig. 5a–c that the maximum load of control beam A1 was 33.4 kN and corresponding compressive strain was 0.0003 mm/mm, while the maximum load of lightweight control beam A2was 30.61 K N and corresponding compressive strain was 0.00538.Ferrocement composite beams showed higher ultimate loads than that of lightweight control beam, A2, and most of them had higher ultimate loads higher than that of normal weight control beam, A1, to different degrees depending on core type, mesh reinforcement type and amount. All corresponding compressive strains to these ultimate loads were higher than that of the normal concrete control beam, A1, and in many cases, higher than those of lightweight control beam A2. This confirms the ductility behaviour studied earlier in phase I. In the next paragraph we will show examples for the comparisons between ferrocement lightweight beams and the control lightweight beam.

For beams with AAC core, beams reinforced by one layer and two layers of expanded metal mesh, B1, and B2 had ultimate loads higher than that of the control lightweight beam A2 by 16% and 32%, respectively. For beams reinforced by two layers and four layers of welded wire mesh, B3, and B4 had ultimate loads higher than that of Beam A2 by 29.2% and 32%, respectively. It was found that the maximum compressive strains for beams in this group was observed for B3, reinforced by two layers of welded wire mesh, and it was higher than that of A2 by 76.6%. For beams with EFC core, beams reinforced by one layer and two layers of expanded metal mesh, G1, and G2 had ultimate loads higher than that of the control lightweight beam A2 by 22.5% and 19%, respectively. For beams reinforced by two layers and four layers of welded wire mesh, G3, and G4 had ultimate loads higher than that of Beam A2 by 1.8% and 4.8%, respectively. The maximum compressive strain in this group was higher than that of control beam A2 by 202% and it was observed for Beam G4 reinforced by four layers of welded wire mesh. For beams with LWC core, beams reinforced by one and two layers of expanded metal mesh, F1, and F2 had ultimate loads higher than that of the control lightweight beam A2 by 33% and 17.7%, respectively. For beams reinforced by two layers and four layers of welded wire mesh, F3, and F4 had ultimate loads higher than that of Beam A2 by 12.7% and 21.7%, respectively. For beams reinforced by three layers and six layers of fiberglass mesh, their ultimate loads were higher than that of Beam A2 by 20% and 26.1%, respectively. It was observed that the maximum compressive strain in this group was higher than that of lightweight control beam A2 by 160.2%, and it was observed for Beam F6 reinforced by six layers of fiberglass mesh. The values in this paragraph shows that the significance of mesh reinforcement type and amount is highly affected by the core type.

5. Theoretical prediction of ultimate loads for test beams

Several studies reported prediction of ultimate loads and ultimate moment capacity for ferrocement structural elements using finite element modelling, empirical solutions and mathematical modelling [26–30]. In this research, the theoretical ultimate moment of the ferrocement beams was calculated in accordance with the method adopted by Fahmyet al. [18]. The basic assumptions adopted in the calculation of the ultimate moment include:

a) Strains in reinforcement, mortar matrix and concrete core are directly proportional to the distances from neutral axis as shown in Fig. 6;
b) Failure occurs when the maximum compressive strain in the ferrocement mortar reaches 0.003;
c) The tensile contribution of mortar matrix and concrete core is neglected at ultimate load and the compressive contribution is represented by a rectangular stress bock of a depth “a” and maximum stress of “$0.67f_{cu}$” (see Fig. 6).

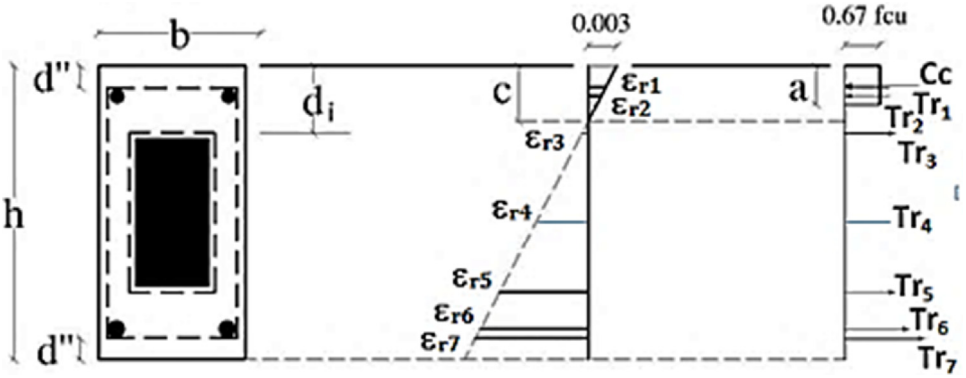

Fig. 6. Strain and forces distribution of ferrocement beam section under bending.

Considering the strain and forces distribution diagram (Fig. 6) at equilibrium,

$$C_c = T \tag{1}$$

$$C_c = \mathrm{a} \times \mathrm{b} \times f_{cu} \tag{2}$$

Where a = 0.80 X c according to the Egyptian code of practice.

$$T = \sum Tr_i = Tr_1 + Tr_2 + Tr_3 + Tr_4 + Tr_5 + Tr_6 + Tr_7 \tag{3}$$

$$Tr_7 = \sigma_{m.bot.} \times A_{m.bot.} \tag{4}$$

$$Tr_6 = \sigma_{st.bot.} \times A_{st.bot.} \tag{5}$$

$$Tr_5 = \sigma_{c.m.bot.} \times A_{c.m.bot.} \tag{6}$$

$$Tr_4 = \sigma_{m.web} \times A_{m.web.} \times No.\,of\ webs \tag{7}$$

$$Tr_3 = \sigma_{c.m.top} \times A_{c.m.top} \tag{8}$$

$$Tr_2 = \sigma_{st.top} \times A_{st.top} \tag{9}$$

$$Tr_1 = \sigma_{m.top} \times A_{m.top} \tag{10}$$

$$Ari = \eta_0 \times V_{fi} \times A_C \tag{11}$$

$$\sigma_{st.bot.} = E_s \times \varepsilon_{s.bot} \le F_{ys}\ if\ (\varepsilon_{s.bot} \le \varepsilon_{y.s.}) \tag{12}$$

$$\sigma_{st.bot.} = F_{ys} + E_{sth} \times (\varepsilon_{s.top} . \varepsilon_{y.s.}) \le F_u\ if\ (\varepsilon_{s.bot} > \varepsilon_{y.s.}) \tag{13}$$

$$\sigma_{st.top} = E_s \times \varepsilon_{s.top.} \le F_{ys}\ if\ (\varepsilon_{s.top.} \le \varepsilon_{y.s.}) \tag{14}$$

$$\sigma_{st.top} = F_{ys} + E_{sth} \times (\varepsilon_{s.top}\, \varepsilon_{y.s.}) \le F_u\ if\ \varepsilon_{s.top} > \varepsilon_{y.s.} \tag{15}$$

$$\sigma_{m.web} = E_s \times \varepsilon_{m.web} \le F_{ym} \tag{16}$$

$$\sigma_{m.bot.} = E_s \times \varepsilon_{m.bot} \le F_{ym} \tag{17}$$

$$\sigma_{m.top} = E_s \times \varepsilon_{m.top} \le F_{ym} \tag{18}$$

Where:

$A_{st.bot.}$ = area of the steel bars at bottom of the beam
$A_{st.top}$ = area of the steel bars at top of the beams
$A_{m.web.}$ = area of the web steel mesh
$A_{c.m.bot.}$ = area of the steel mesh wrapping bottom of the core

$A_{c.m.top}$ = area of the steel mesh wrapping top of the core
$A_{m.bot.}$ = area of the bottom steel mesh
$A_{m.top}$ = area of the top steel mesh
Ari = effective area of reinforcement either mesh or skeletal bars
η_0 = efficiency factor of reinforcement in the loading direction
A_C = cross section area of ferrocement composite section
a = depth of the compression block in the ferrocement matrix
b = width of the specimen
C = neutral axis depth from the top of the specimen
E_s = modulus of elasticity of the steel
E_{sth} = strain-hardening modulus of the steel
F_{ym} = yield stress of the steel mesh
F_u = ultimate strength of the steel mesh
f_{cu} = characteristic compressive strength of ferrocement mortar matrix
C_c = Internal forces in compression zone
T_r = Internal forces in tension zone

The strain at the top steel bars, bottom steel bars, web steel reinforcement mesh and bottom steel reinforcement mesh, $\varepsilon_{s.top}$,$\varepsilon_{s.bot}$,$\varepsilon_{m.web}$, $\varepsilon_{m.bot}$, $\varepsilon_{m.top}$, can be obtained from the geometry of the strain distribution shown in Fig. 6. Strains, $\varepsilon_{s.\,top}$ and $\varepsilon_{s.\,bot}$ could be tension (+ve sign) or compression (-ve sign) depending on the location of the neutral axis. The trial and error method performed using computer spreadsheet was used to determine the location of the neutral at a distance C from the top fibre. Once the neutral axis has been located, calculating the ultimate moment (M_u) of a section can be done by taking moment about the point of application of the compressive force as follows:

$$M_u = \sum Tr_i \times (d_i - C/2) \tag{19}$$

The ultimate load (P_{ui}) can be determined from Eq. (20) which represents a simply supported beam subjected to central concentrated load.

$$M_u = \frac{P_{u1}}{4} \times L_{effective} \tag{20}$$

Where $L_{effective}$ = the effective span of the test specimen
P_{u1} = the ultimate load for flexure failure

Considering the shear failure of the specimen, the ultimate shear strength, Q_u, of the different designations was calculated using Eq. (21) below:

$$Q_u\,(0.24\sqrt{f_{cu}})\,Bd + F_{ym}\,A_{meshweby}\,N \tag{21}$$

$$P_{u2} = 2Q_u \tag{22}$$

Where d = the effective depth of the beam
$A_{meshweby}$ = the cross-sectional area of the web mesh reinforcement in the vertical direction within a length equal to (d)
N = number of webs
P_{u2} = the ultimate load for shear failure

For the case of specimens with light brick core and extruded foam, the shear strength of the light brick and foam was considered negligible. Eq. (21) is based on the shear strength of beams in accordance to the CEN [26]. The web mesh reinforcement contribution has been incorporated in the CEN, code equation [26] as a replacement to the effect of the stirrups. The failure load and failure mode of the beams are determined by the smallest of $P_{u1}$and P_{u2}. The failure mode is by flexure if $P_{u1}$is the smaller of the two values, otherwise, the failure mode is by shear. The respective ultimate load for each specimen was calculated from their geometric and material properties. It can be found from the calculations through Eqs. (20) and (22), and from observation of crack pattern (see Fig. 4) that the failure mode of all the studied beams was flexure except for Beam F2 which failed in shear. This may be explained by increasing number of ferrocement layers for Beam F2 which enhanced its flexural stiffness and that's why it failed in shear [19]. Table 1 presents the experimental to predicted ratios for ultimate loads of the studied beams. It can be seen from the table that the theoretical ultimate loads are in reasonable agreement with the experimental values for most of the studied beams. The highest ratios were for beams F1 and F4 which were made of LWC core material, which is considered as acceptable agreement. The ratio of the experimental ultimate load to the predicted one ranged from 0.91 to 1.26.

6. Conclusions

This is phase II of the research carried out by the authors to investigate the effect of filling core, and mesh reinforcement type and amount on the structural behaviour of lightweight ferrocement composite beams. The following conclusions can be drawn from the observations of the experimental results and the theoretical prediction:

1 Core type, mesh reinforcement type and number of mesh layers have significant effect on the studied structural indicators to different degrees. The different studied structural indicators showed improvement over those of lightweight control beam. However, sensitivity of structural indicators to core types, mesh types and amount varies from elastic stage of load-deflection to post-cracking stage. When using expanded metal mesh, higher post-cracking loads were exhibited compared to those beams reinforced by welded wire mesh regardless of the core filling type. For post cracking load indicator, confinement with expanded metal mesh was the decisive factor affecting the post-cracking load capacity.
2 The studied ferrocement beams generally exhibited higher pre-crack stiffness when compared to the light weight control specimen. Most of ferrocement beams exhibited higher serviceability loads compared to the control specimens. However, specimens reinforced with expanded metal mesh mostly reached their serviceability loads before the initiation of first crack while other specimens reinforced with welded wire mesh developed first crack prior to reaching their serviceability load. Beams reinforced with expanded metal mesh mostly exhibit higher post-cracking load compared to those reinforced with welded wire mesh.
3 Energy absorption values of studied ferrocement beams were, generally, higher than that of the lightweight control specimen. The highest energy absorption property was shared between beams made of AAC and LWC cores and the lowest was found mostly with beams made of EFC core. In addition, energy absorption was found the highest in beams reinforced with expanded metal mesh among the groups.
4 Lightweight control specimen and all the ferrocement beams showed higher ultimate load-to-weight ratios compared to the normal concrete control specimen. The core material and mesh reinforcement had a significant effect on such ratios. Ferrocement beams of cores made of AAC and EFC exhibited the highest ultimate load-to-weight ratios while the lowest was observed in beams made of LWC core. Moreover, while increasing the number of mesh reinforcement layers showed better strength among the ferrocement beams made of AAC core regardless the mesh type, this was not necessarily the case with beams made of EFC and LWC cores.
5 Theoretical calculations, based on the assumption of strains and forces distribution block, were carried out to predict the ultimate loads for the studied beams. It was found that the predicted results are in a reasonable agreement with the experimental values. The ratio of the experimental ultimate load to the theoretical value ranged from 0.91 to 1.26. The adopted theoretical approach may be used as a design methodology for ferrocement elements.
6 Results showed that ferrocement composite beams with different core types and reinforced with several layers of mesh reinforcement may be used as an alternative to traditional reinforced normal concrete or lightweight beams in several applications. However, choosing the type of mesh reinforcement is important for a specific application. For example, beams reinforced by expanded metal mesh with narrower crack width, showed higher post-cracking loads compared to those reinforced by welded wire mesh which makes expanded metal mesh more suitable for water structures. In addition, the use of expanded metal mesh in ferrocement is recommended to protect structural elements against disasters such as earthquakes or fire because of its higher energy absorption and fire resistance compared to welded wire mesh.

References

[1] ACI 549.1R-93 & ACI 549-1R-88, Guide for the Design Construction, and Repair of Ferrocement, ACI Comm. 549.1R-93; ACI 549-1R-88 1R-93. American c (1997).
[2] I.G. Shaaban, O. Seoud, Experimental behaviour of full-scale exterior beam-column space joints retrofitted by ferrocement layers under cyclic loading, Case Stud. Constr. Mater. 8 (June) (2018) 61–78, doi:http://dx.doi.org/10.1016/j.cscm.2017.11.002.
[3] F. Matalkah, H. Bharadwaj, P. Soroushian, W. Wu, A. Almalkawi, A.M. Balachandra, A. Peyvandi, Development of sandwich composites for building construction with locally available materials, Constr. Build. Mater. 147 (2017) 380–387, doi:http://dx.doi.org/10.1016/j.conbuildmat.2017.04.113.
[4] O. Lalaj, Y. Yardım, S. Yılmaz, Recent perspectives for ferrocement, Res. Eng. Struct. Mat 1 (2015) 11–23, doi:http://dx.doi.org/10.17515/resm2015.04st0123.
[5] E.L. Elsayed, Structural Behaviour of Light Weight Ferrocement Composite Concrete Beams an MSc Thesis submitted to Faculty of Engineering, Benha University, 138pp, (2014) .
[6] A. Leeanansaksiri, P. Payakapo, A. Ruangrassamee, Seismic capacity of masonry infilled RC frame strengthening with expanded metal ferrocement, Eng. Struct. 159 (2018) 110–127, doi:http://dx.doi.org/10.1016/j.engstruct.2017.12.034.
[7] A.E. Naaman, Ferrocement: progress review and critical need for the future, 11th International Symposium on Ferrocement and Textile Reinforced Concrete 3rd ICTRC, pp. 9–14. proceedings pro 098: FERRO-11-11th International Symposium On Ferrocement and 3rd ICTRC International Conference On Textile Reinforced Concrete, (2018) .
[8] W. Al-Rifai, K.A. Mohammad, Strength of ferrocement-brick composite columns, J. Ferrocement 30 (2000) 69–83.
[9] S. Wasim, N. Razvi, Review on ferrocement, Int. J. Innov. Eng. Technol. (IJIET) 6 (2015) 338–340.
[10] G. Singh, Singh J. Dhanoa, R. Singh, Retrofitting of reinforced concrete beam by ferrocement technique, Indian J. Sci. Technol. 9 (2016), doi:http://dx.doi.org/10.17485/ijst/2016/v9i15/88243.
[11] W.N. Al-Rifaei, A.H. Hassan, Structural behavior of thin ferrocement one-way bending elements, J. Ferrocement 24 (1994) 115–126.
[12] M.A. El-Wafa, K. Fukuzawa, Flexural behavior of lightweight ferrocement sandwich composite beams, J. Sci. Technol. 15 (2010) 3–16.
[13] A.M. Noor, R.S. Salihuddin, R. Mahyuddin, Ferrocement encased lightweight aerated concrete: a novel approach to produce sandwich composite, J. Mater. Lett. 61 (2007) 4035–4038.
[14] T. Chandrasekhar, T.D. Rao, Gunneswara Rao, Ramana N.V. Rao, An experimental study on ferro cement channel units under flexural loading, Int. J. Mech. Solids 3 (2008) 195–203.
[15] I.G. Shaaban, Expanded wire fabric permanent formwork for improving flexural behaviour of reinforced concrete beams, Composite Materials in Concrete Construction: Proceedings of the International Seminar held at the University of Dundee (2002) 59–70, doi:http://dx.doi.org/10.1680/cmicc.31746.0006.
[16] M. Abdul Kadir, A. Abdul Samad, Z. Che Muda, A. Ali, Flexural behavior of composite beam with ferrocement permanent formwork, J. Ferrocement 27 (1997) 209–214.
[17] A. Abdel Tawab, E.H. Fahmy, Yb. Shaheen, Use of permanent ferrocement forms for concrete beam construction, Mater. Struct. 45 (2012) 1319–1329.

[18] E.H. Fahmy, Y.B.I. Shaheen, A.M. Abdelnaby, M.N. Abou Zeid, Applying the ferrocement concept in construction of concrete beams incorporating reinforced mortar permanent forms, Int. J. Concr. Struct. Mater. 8 (2014) 83–97, doi:http://dx.doi.org/10.1007/s40069-013-0062-z.
[19] I.G. Shaaban, Y.B. Shaheen, E.L. Elsayed, O.A. Kamal, P.A. Adesina, Flexural Characteristics of lightweight ferrocement beams with various types of core materials and mesh reinforcement, Constr. Build. Mat. J.l 171 (May) (2018) 802–816, doi:http://dx.doi.org/10.1016/j.conbuildmat.2018.03.167.
[20] European Committee for Standardization, CEN, Eurocode 2: Design of Concrete Structures - Part 1: General Rules and Rules for Buildings Brussels, pp. 26–35 & 132, (2002) .
[21] Y.B.I. Shaheen, A.A. Elsayed, Design and construction of ferrocement water tanks, Concrete Research Letters 4 (December (4)) (2013) 684–695.
[22] Er. Mandeep Singh, Er. Mohit Talwar, Ferrocement as a construction material, Int. J.Adv. Res. Comput. Sci. 8 (May (4)) (2017). (Special Issue), REVIEW ARTICLE, ISSN No. 0976-5697 www.ijarcs.info.
[23] R.F. Hassan, Flexural and shear behaviour of RC concrete beams reinforced with Fiber wire mesh, J. Univ. Babylon Eng. Sci. 26 (February (3)) (2018) 264–273.
[24] D.G. Gaidhankar, M.S. Kulkarni, Abhay R. Jaiswal, Ferrocement composite beams under flexure, International Research Journal of Engineering and Technology (IRJET) 4 (October (10)) (2017) 117–124 e-ISSN: 2395-0056.
[25] Y.B.I. Shaheen, E.A. Eltehawy, Structural behaviour of ferrocement channels slabs for low cost housing, Chall. Concr. Res. Lett. J. 8 (2017) 48–64.
[26] A.H. Gandomi, D.A. Roke, K. Sett, Genetic programming for moment capacity modeling of ferrocement members, Eng. Struct. 57 (2013) 110–127, doi: http://dx.doi.org/10.1016/j.engstruct.2013.09.022 2013.
[27] S.N. Mhadeshwar, A.M. Naik, Experimental performance, mathematical modelling and development of stress block parameter of ferrocement beams with rectangular trough shaped skeletal steel, Int. Res. J. Eng. Technol. (IRJET) 4 (June (6)) (2017) 1387–1393 e-ISSN: 2395-0056.
[28] H. Eskandari, A. Madadi, Investigation of ferrocement channels using experimental and finite element analysis, Eng. Sci. Technol. Int. J. 18 (2015) 769–775. http://creativecommons.org/licenses/by-nc-nd/4.0/.
[29] A.A. Shaheen, A.M. Torkey, I.G. Shaaban, Influence of reinforcement orientation on the behaviour of ferrocement slabs, J. Egypt. Soc. Eng. 37 (1) (1998) 9–14.
[30] I.G. Shaaban, Behaviour of thin plates reinforced with wire fabric, Ain Shams Univ. Sci. Bull. 32 (December (4)) (1997) 21–40.